Journal of Neuroscience Research 79:383–391 (2005)

Elevated Endogenous GABA Level Correlates with Decreased fMRI Signals in the Rat Brain During Acute Inhibition of GABA Transaminase

Zhengguang Chen,[1] Afonso C. Silva,[2] Jehoon Yang,[1] and Jun Shen[1]*
[1]Molecular Imaging Branch, NIMH, Bethesda, Maryland
[2]Laboratory of Functional and Molecular Imaging, NINDS, Bethesda, Maryland

Vigabatrin and gabaculine, both highly specific inhibitors of GABA (γ-aminobutyric acid) transaminase, cause significant elevation of endogenous GABA levels in brain. The time course of GABA concentration after acute GABA transaminase inhibition was measured quantitatively in the α-chloralose-anesthetized rat brain using in vivo selective homonuclear polarization transfer spectroscopy. The blood oxygenation level-dependent (BOLD) effect in functional magnetic resonance imaging (fMRI) has been considered to be coupled tightly to neuronal activation via the metabolic demand of associated glutamate transport. Correlated with the rise in endogenous GABA level after vigabatrin or gabaculine treatment, the intensity of BOLD-weighted fMRI signals in rat somatosensory cortex during forepaw stimulation was found to be reduced significantly. These results are consistent with previous findings that inhibition of GABA transaminase leads to augmented GABA release and potentiation of GABAergic inhibition.

Key words: functional imaging; in vivo spectroscopy; vigabatrin; gabaculine

γ-Aminobutyric acid (GABA) is the major inhibitory neurotransmitter in the mammalian cortex (McCormick, 1989). GABA is synthesized from its metabolic precursor glutamate in a single α-decarboxylation step catalyzed by glutamate decarboxylase (GAD) (Martin and Rimvall, 1993). GABA is catabolized to succinic semialdehyde and then to succinate by the sequential actions of GABA transaminase (GABA-T) and succinic semialdehyde dehydrogenase (SSADH) (Jung et al., 1977). When GABA-T is inhibited by its irreversible inhibitors such as vigabatrin (γ-vinylGABA) or gabaculine, there is substantial accumulation of both cytosolic and vesicular GABA in the brain (Jung et al., 1977; Iadarola and Gale, 1981; Loscher, 1982; Mattson et al., 1994; Preece and Cerdan, 1996). In cell culture studies, GABA-T inhibition has been shown to enhance depolarization-evoked release of endogenous GABA (Wood et al., 1988; Wu et al., 2001). Similarly, increased electrical stimulation-evoked GABA release has also been observed in brain slices treated with GABA-T inhibitors (Kihara et al., 1988). In studies in vivo, elevated GABA levels in brain, generated by administration of vigabatrin or gabaculine or by transplanted genetically engineered GABA-producing cells, have been found to correlate with protection against experimentally induced seizures in rodents (Loscher, 1982; Bernasconi et al., 1988; Gernert et al., 2002). Increased presynaptic availability and GABA release resulting from GABA-T inhibition are believed to cause the anticonvulsive effects of vigabatrin and gabaculine (Iadarola and Gale, 1981; Jackson et al., 1994; Golan et al., 1996). Vigabatrin has also been shown to have anxiolytic and antipanic properties (Sherif et al., 1994; Dalvi and Rodgers, 1996). Recently, it has been reported that increasing GABA levels in rostral agranular insular cortex using either vigabatrin or gene transfer mediated by a GAD67-encoding viral vector leads to elevated nociceptive threshold, producing long-term analgesia in rats (Jasmin et al., 2003).

Clinical studies have demonstrated that vigabatrin is an effective anticonvulsant drug in drug-resistant partial epilepsy, with the elevated GABA concentration in the brain correlating with improved seizure control (Ben-Menachem et al., 1989; Riekkinen et al., 1989; Petroff et al., 1996). The inhibition of GABA-T by vigabatrin leads to augmented presynaptic availability and release of endogenous GABA and therefore reduced cortical excitability, which has been considered the mechanism by which vigabatrin exerts its anticonvulsant action in epileptic patients (Schechter and Sjoerdsma, 1990; Schousboe et al., 1990). Vigabatrin has also been shown to depress cerebral metabolic rate for glucose (CMR_{Glc}) and cerebral blood flow (CBF) in epileptic patients as measured with ^{18}F-

*Correspondence to: Jun Shen, PhD, Molecular Imaging Branch, National Institute of Mental Health, Bldg. 10, Rm. 2D51A, 9000 Rockville Pike, Bethesda, MD 20892-1527. E-mail: shenj@intra.nimh.nih.gov

Received 6 July 2004; Revised 8 October 2004; Accepted 11 October 2004

Published online 23 December 2004 in Wiley InterScience (www.interscience.wiley.com). DOI: 10.1002/jnr.20364

fluorodeoxyglucose and ^{15}O-water positron emission tomography (PET). The decrease in CMR_{Glc} was found to correlate with the increase in total cerebrospinal fluid (CSF) GABA concentration (Spanaki et al., 1999).

In vivo functional magnetic resonance imaging (fMRI) measures the brain's hemodynamic responses to neuronal activation, including the susceptibility-based blood oxygenation level-dependent (BOLD) image contrast and the change in regional CBF (rCBF) (van Zijl et al., 1998; Silva et al., 1999; Silva and Koretsky, 2002). Both effects are highly coupled to neuronal activities (Hoge et al., 1999; Ogawa et al., 2000; Logothetis et al., 2001; Silva and Koretsky, 2002). BOLD fMRI signal changes in response to activation stimuli are accompanied by an increase in regional oxygen consumption and rCBF. The increase in rCBF exceeds the increase in oxygen consumption; consequently, there is a reduction in regional concentrations of deoxyhemoglobin, which acts as an endogenous susceptibility contrast agent. The increase in regional signal intensity caused by a reduction of deoxyhemoglobin forms the basis of the BOLD effect. fMRI techniques have been applied recently to pharmacologic studies of animal models (Silva et al., 1995; Marota et al., 2000), providing a powerful tool for studying the kinetics of drug effects. Similar to PET, fMRI could be a very useful in vivo tool for assessing the role of GABA metabolism and GABAergic activities in the control of cortical excitability. Complementary to fMRI, magnetic resonance spectroscopy (MRS) allows in vivo measurement of regional cerebral concentration of GABA (Shen et al., 2002a; Shen, 2003; Choi et al., 2004). The kinetics of GABA synthesis after vigabatrin or gabaculine treatment can be monitored using in vivo MRS (Behar and Boehm, 1994; Mattson et al., 1994; Petroff et al., 1996; Shen et al., 2004).

In the present work, fMRI and MRS were combined to study the effects of acute GABA-T inhibition on the hemodynamic response to somatosensory stimulation in α-chloralose anesthetized rats. It was hypothesized that increased endogenous GABA should decrease the intensity of the BOLD response to somatosensory stimulation. fMRI experiments were carried out to characterize the changes in BOLD-weighted fMRI signal after vigabatrin treatment. The time course of GABA concentration in the rat cortex after acute vigabatrin administration was measured using quantitative in vivo MRS. Results indicated a significant correlation between increases in GABA concentration as measured by MRS and the decrease in the BOLD response as measured by fMRI. To corroborate such findings, experiments were also repeated using gabaculine (Rando, 1977; Wood et al., 1982; Patel et al., 2001) for acute GABA-T inhibition.

MATERIALS AND METHODS

Animal Preparation

Male adult Sprague-Dawley rats (185 ± 25 g) were orally intubated and mechanically ventilated with a mixture of 70% N_2/30%O_2 and 1.5% isoflurane. A femoral artery and a femoral vein were cannulated for monitoring arterial blood gases (pO_2, pCO2), pH, arterial blood pressure, and for intravenous infusion of α-chloralose (initial dose 80mg/kg supplemented with a constant infusion of 26.7 mg/kg/hr throughout the experiment) and for acute vigabatrin (500 mg/kg, 0.6 cc; Sigma-Aldrich, St. Louis, MO) or gabaculine (100 mg/kg, 0.6 cc, BIOMOL Research Laboratories, Inc.) administration. Untreated animals served as controls. For the control group, saline instead of vigabatrin or gabaculine was injected i.v. After surgery, isoflurane was discontinued and pancuronium bromide was administered (2 mg/kg every 90 min i.v.) for immobilization. All physiologic parameters were kept within the normal limits: arterial blood pO_2 was within 120–150 mmHg, pCO_2 within 25–35 mm Hg, mean arterial blood pressure within 180 ± 30 mm Hg (a transient ~20% decrease in mean arterial blood pressure was observed upon acute gabaculine injection, which was reversed quickly and did not reoccur), and plasma pH within 7.35–7.45. Ventilation and plasma pH were adjusted based on periodic blood sampling. Rectal temperature was monitored during scanning and maintained at ~37°C with heated circulating water. End-tidal CO_2, tidal pressure of ventilation, and heart rate were also monitored. For fMRI studies, both forepaws were stimulated through needles inserted in between digits 1, 2 and digits 3, 4. The needles were connected to an electrical simulator that generated pulses (2 mA, 0.3 msec) at a frequency of 3 Hz (Silva et al., 1999; Silva and Koretsky, 2002). All experiments were carried out under protocols approved by NIMH Animal Care and Use Committee.

fMRI Experiments

Nuclear magnetic resonance (NMR) experiments were carried out on two 11.7 Tesla Bruker AVANCE spectrometers (Bruker Billerica, MA) with either a 31-cm inner diameter (i.d.) horizontal bore magnet or 8.9-cm i.d. vertical bore magnet (Magnex Scientific, Abingdon, UK). The NMR probe consisted of either an actively decoupled volume coil transmission (5-cm i.d.)/surface coil (1.5-cm i.d.) reception system or a surface transceiver coil (1.5-cm i.d.). The surface coils were centered 0–1 mm rostral to bregma. Three-slice (coronal, horizontal, and sagittal) scout rapid acquisition with relaxation enhancement (RARE) images were used to position the rat inside the magnet. For fMRI studies, three-slice single-shot coronal spin-echo echo planar imaging (EPI) was used to measure BOLD-weighted fMRI responses to forepaw stimulation in the primary somatosensory cortex (slice thickness = 2 mm; field of view [FOV] = 2.56 cm with a 64 × 64 matrix corresponding to an in-plane resolution of 400 μm × 400 μm; repetition time/echo time [TR/TE] = 500–1,000/25 msec). The stimulation paradigm consisted of an initial 15–30-sec baseline period followed by a 20–-sec stimulation period and finalized with a 15–30-sec baseline period.

In Vivo GABA Editing

For spectroscopy studies, a 4.5 mm × 2.5 mm × 4.5 mm voxel located inside the EPI slice package was selected and shimmed using FASTMAP/FLATNESS (Gruetter, 1993; Shen et al., 1999a; Chen et al., 2004) to correct all first-order, all second-order, and the z^3, z^2x shims. An adiabatic point-resolved spectroscopy (PRESS) sequence (Chen et al., 2004) was used to

obtain a short-TE scout spectrum and to measure the resonance frequency of the creatine methyl group from the selected voxel (number of scans (NS) = 64–256; TR/TE = 2,000/15 msec). The pulse sequence used a 90-degree adiabatic half-passage pulse (1 msec) for excitation and six 180-degree slice-selective adiabatic hyperbolic secant pulses (μ = 5, 2 msec) for three-dimensional spatial localization. Chemical shift selective (CHESS) pulses were used for water suppression.

A one-dimensional selective homonuclear polarization transfer method (Shen et al., 2004) was used to acquire edited GABA spectra (NS = 256; TR/TE = 2,000/68 msec). Briefly, the thermal equilibrium GABA-4 signal at 3.0 parts per million (ppm) and the overlapping creatine, glutathione, and macromolecules were suppressed completely in a single-shot using CHESS. The edited 3.0-ppm GABA peak was then generated anew from the thermal equilibrium GABA-3 signal at 1.91 ppm via homonuclear polarization transfer. Single-shot spatial localization was achieved using a five-lobe sinc (0.5 msec) for slice-selective excitation along the x-dimension and slice-selective adiabatic hyperbolic secant pulses (μ = 5, 2 msec) for spatial localization along the y- and z-dimensions. The J evolution between GABA-2 and GABA-3 was refocused using a 15-msec (B_1 = 375 Hz) double-band numerically optimized 180-degree Hermite-based pulse during the preparation of GABA-3 and GABA-4 antiphase coherence (Shen et al., 1999b; Shen et al., 2002a). The final GABA-4 spin state before data acquisition was $(I_y + I'_y + 4I_yS_zS'_z + 4I'_yS_zS'_z)/2$, which represents the full intensity of the outer two lines of the GABA-4 triplet under the weak coupling approximation. The double-band optimized Hermite-based pulse also generated minimal excitation of the macromolecules at 1.72 ppm, leading to negligible macromolecule contamination to the regenerated GABA-4 at 3.0 ppm, which was verified using a metabolite null experiment. The intense signal from N-acetyl asparate (NAA) methyl group at 2.02 ppm in the edited GABA spectra served as an internal reference for zero-order phase and concentration.

In Vitro Experiments

To quantify the cerebral GABA concentration, the metabolism of the rat brain was arrested using a microwave fixation system (Model TMW-6402C; Muromachi Kikai Co., Tokyo, Japan) immediately after in vivo spectroscopy data acquisition. The microwave system inactivates enzymatic processes in ~1 sec without affecting the level or the distribution of GABA (Tappaz et al., 1977; Ishikawa et al., 1983; Miller et al., 1990). The rat was then decapitated. The brain tissue corresponding to the spectroscopy voxel was removed and weighed. Extraction using perchloric acid (PCA) (12%, 3–4 ml/g) was carried out as described previously (Dimitrijevic et al., 2001; Patel et al., 2001). Brain extracts were centrifuged at 13,000 rpm for 20 min at 4°C. The filtered supernatant was repeatedly lyophilized and redissolved in D_2O (pH 7.4). GABA concentrations at the end of in vivo spectroscopy data acquisition were measured using standard high-resolution pulse-acquire experiment (NS = 4,096; TR/TE = 6,000/0 msec; flip angle = 45 degrees) in D_2O on the vertical widebore 11.7 Tesla spectrometer using a 2.5-mm broadband inverse probe. As an internal standard for chemical shift, 3-(trimethylsilyl) propionic-2,2,3,3-d_4 acid (TSP-d_4) was added.

Data Analysis

The EPI Nyquist ghosts were corrected based on a one-dimensional phase modulation of the spectra of even or odd echoes derived from the imaging data (Buonocore and Gao, 1997). Activation maps were generated using the STIMULATE software (written by J.P. Strupp, University of Minnesota, Minneapolis, MN) from pixels presenting a minimum cross-correlation coefficient (CCC; Bandettini et al., 1993) of 0.3. To compare relative fMRI signal changes in the somatosensory cortex, regions of interest (a cluster of 4 × 4 pixels) were chosen based on the center of the highest intensity in activation maps on both sides of the cortex. Student's *t*-tests were carried out to compare differences in fMRI signal intensities. Spectroscopy data were processed using XWINNMR v3.1 software (Bruker-Biospin, Billerica, MA). In vigabatrin- or gabaculine-treated rats, the concentration of GABA as a function of time was calculated based on the in vivo intensity of the edited GABA peak at 3.0 ppm and the concentration of GABA at the end point measured from PCA extracts assuming the concentration of total NAA is 9.4 μmol/g wet weight (Pfeuffer et al., 1999). The time course of GABA concentration after vigabatrin treatment was fitted to the following exponential equation:

$$[\mathrm{GABA}](t) = [\mathrm{GABA}]_0 \exp(-t/t_{1/2}) + [\mathrm{GABA}]_\infty (1 - \exp(-t/t_{1/2})) \quad (1)$$

where $t_{1/2}$ is the halftime of the exponential function, $[\mathrm{GABA}]_0$ and $[\mathrm{GABA}]_\infty$ are the initial and equilibrium GABA concentration. The time course of GABA concentration after gabaculine treatment was fitted to a linear equation (Behar and Boehm, 1994).

RESULTS

Effect of Acute Vigabatrin Administration on BOLD-Weighted fMRI Signals

EPI images of a control rat and those of a vigabatrin-treated rat were compared in Figure 1. The activation maps were overlaid on the single-shot EPI images per se. As seen in Figure 1, in contrast to the control, acute vigabatrin administration (500 mg/kg, 0.6 cc i.v.) produced specific BOLD-weighted fMRI signal changes manifested as a general decrease in both the volume of activated tissue and the intensity of the response to forepaw stimulation. Figure 2 shows the temporal effects of vigabatrin (shaded bar, 500 mg/kg, 0.6 cc i.v.; n = 11) and saline (blank bar, 0.6 cc i.v.; n = 5) administration on the relative % changes in fMRI signal intensity. For each time point, the fMRI signal from the selected cluster of 4 × 4 pixels was averaged over the duration of forepaw stimulation. In contrast to the control group, the vigabatrin-treated group showed a gradual decrease in the intensity of the fMRI response. At the 30-min point after vigabatrin administration, the relative changes in fMRI signal between the two groups started to differ with statistical significance ($P < 0.01$). Before this point, differences in the changes in fMRI signal between the two groups were not statistically significant ($P > 0.20$). Five vigabatrin-

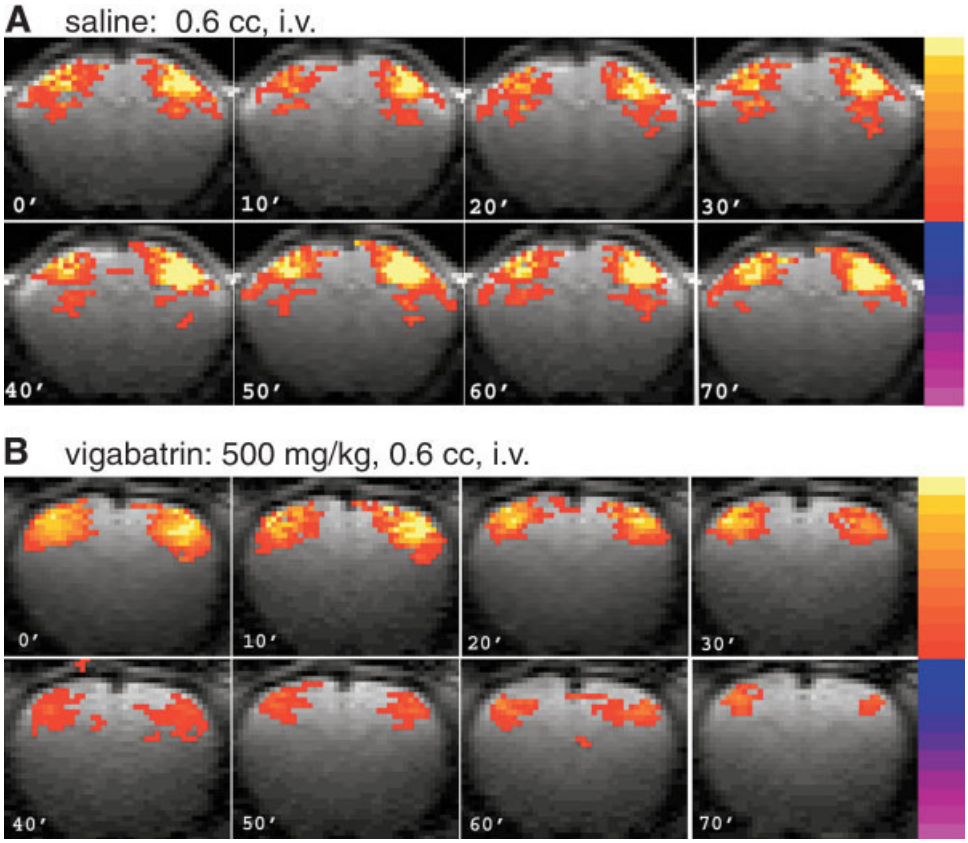

Fig. 1. Time points from a set of coronal EPI images of a control rat (**A**) and a vigabatrin-treated rat (**B**; 500 mg/kg, 0.6 cc i.v.) obtained during forepaw stimulation (slice thickness = 2 mm; field of view [FOV] = 2.56 cm with a 64 × 64 matrix corresponding to an in-plane resolution of 400 μm × 400 μm; repetition time/echo time (TR/TE) = 500–1,000/25 msec. The slice was centered approximately 0–1 mm rostral to bregma. The activation maps were overlaid on the single-shot EPI images from which the activation maps were generated. The acute vigabatrin administration produced BOLD-weighted fMRI signal changes manifested as a general decrease in both the volume of activated tissue and the intensity of the response to forepaw stimulation.

treated rats were also measured for up to 140 min after vigabatrin administration, and the depression in fMRI responses was found to be sustained. Because no time-matched data from the control group were acquired, those fMRI data were not included in the statistical analysis.

Effect of Acute Vigabatrin Administration on Cerebral GABA Concentration

Figure 3A shows typical in vivo MR spectra of the GABA-4 signal at 3.0 ppm edited using the one-dimensional homonuclear polarization transfer method at different points after acute vigabatrin treatment (500 mg/kg, 0.6 cc i.v.; $n = 5$). A clear doublet consistent with the theoretically derived GABA-4 spin state was observed in all spectra acquired, indicating minimal contamination from other signals. No statistically significant changes in the concentration of other metabolites were found in either the unedited short-TE (15 msec) PRESS spectra over the duration of the in vivo experiment or in the high-resolution spectra of the PCA extracts (data not shown). Figure 3B shows a plot of the cerebral GABA concentration as a function of time after acute vigabatrin administration, with the solid line indicating the temporal fit according to equation (1). From the exponential fit, the halftime ($t_{1/2}$) = 110 ± 33 min (mean ± SD, $n = 5$) and $[GABA]_\infty$ = 3.1 ± 0.7 μmol/g wet weight (mean ± SD, $n = 5$). $[GABA]_0$ = 1.2 ± 0.1 μmol/g wet weight (mean ± SD, $n = 11$) (Shen et al., 2004), determined from rats without vigabatrin or gabaculine administration, was used in the exponential fit.

Effects of Acute Gabaculine Administration

Acute gabaculine administration (100 mg/kg, 0.6 cc i.v.; $n = 7$) also produced a general decrease in both the volume of activated tissue and the intensity of the response to forepaw stimulation in the BOLD-weighted fMRI maps. The temporal effects of gabaculine on the relative changes in fMRI signal (in % change of fMRI signal) were analyzed. For each point, the fMRI signal from the selected cluster of 4 × 4 pixels was averaged over the duration of forepaw stimulation. At the 20-min point after gabaculine administration, the relative changes in fMRI signal between the control group and the gabaculine-treated group started to differ with statistical significance ($P < 0.01$). At 70 min, an averaged ~65% decrease in fMRI signal was observed as compared to that before gabaculine injection. The cerebral concentration of GABA as a function of time was also measured using the in vivo selective homonuclear polarization transfer method for up to 2.5 hr after acute gabaculine administration (100 mg/kg, 0.6 cc i.v.; $n = 5$). The concentration of GABA as a function of time was fitted to a linear equation. From least-square linear regression analysis, $\Delta[GABA]/\Delta t$ was

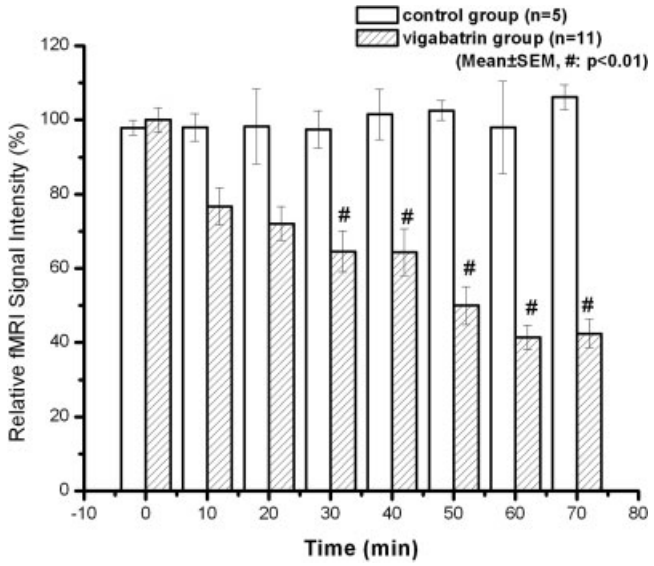

Fig. 2. The temporal effects of vigabatrin administration on the relative changes in BOLD-weighted fMRI signal. For each time point, the fMRI signal from the selected cluster of 4 x 4 pixels was averaged over the duration of forepaw stimulation. Shaded bar, vigabatrin-treated group (500 mg/kg, 0.6 cc i.v.; $n = 11$); blank bar, control group (saline, 0.6 cc i.v.; $n = 5$). In contrast to the control group, the vigabatrin-treated group showed a gradual decrease in the intensity of the fMRI response. At the 30-min point after vigabatrin administration, the relative changes in fMRI signal between the two groups started to differ with statistical significance ($P < 0.01$). Before this point, differences in the changes in fMRI signal between the two groups were not statistically significant ($P > 0.20$).

determined to be 0.020 ± 0.005 μmol/g wet weight/min (mean ± SD, $n = 5$).

Correlation between BOLD-Weighted fMRI Signal Intensity and Cerebral GABA Concentration

The concentrations of GABA as a function of time after vigabatrin or gabaculine treatment determined using in vivo MRS in separate groups of rats were fitted to an exponential or linear function as described above. The concentrations of GABA during the course of fMRI measurement in vigabatrin- or gabaculine-treated rats were calculated from the fits to the posttreatment time course of GABA concentration. For vigabatrin treatment, [GABA](t) = (1.2 μmol/g wet weight) (exp[−t/110 min]) + (3.1 μmol/g wet weight)(1 − exp[−t/110 min]) was used. For gabaculine treatment, [GABA](t) = 1.2 μmol/g wet weight + (0.020 μmol/g wet weight/min)(t) was used. The relative changes in fMRI signal intensities due to vigabatrin or gabaculine treatment were plotted in Figure 4 as a function of endogenous GABA concentration during acute inhibition of GABA-T. As shown in Figure 4, the reduction in the brain BOLD response to somatosensory stimulation clearly correlates with the increase in endogenous GABA concentration after acute vigabatrin or gabaculine administration.

DISCUSSION

The basal GABA concentration in rat brain measured using in vivo selective homonuclear polarization transfer spectroscopy was 1.2 ± 0.1 μmol/g wet weight (mean ± SD, $n = 11$), which is in agreement with previous neurochemical measurements using microwave fixation for instantaneous inactivation of brain metabolism (Tappaz et al., 1977; Miller et al., 1990). Higher basal brain GABA concentrations measured using decapitation and rapid freezing with liquid nitrogen, which have been reported previously in the literature (Miller et al., 1990), have been attributed to rapid postmortem GABA anabolism. The GABA concentration in α-chloralose-anesthetized rat brain increased significantly upon acute administration of vigabatrin (Fig. 3). The GABA accumulation after acute vigabatrin administration (500 mg/kg, 0.6 cc i.v.) extrapolated from equation (1), and the $[GABA]_0$, $[GABA]_\infty$ and $t_{1/2}$ values measured in this study are in agreement with the range of values reported previously using similar dosage of vigabatrin (Jung et al., 1977; Manor et al., 1996; Errante and Petroff, 2003). Gabaculine is a more potent GABA-T inhibitor than vigabatrin. Correspondingly, we found that the rate of GABA accumulation after 100 mg/kg intravenous injection of gabaculine was 0.020 ± 0.005 μmol/g wet weight/min, which is in agreement with previous in vivo MRS measurements using a similar intravenous administration protocol (Behar and Boehm, 1994).

Correlated with the spectroscopic results, our functional imaging data demonstrated that acute vigabatrin (500 mg/kg, 0.6 cc i.v.) or gabaculine (100 mg/kg, 0.6 cc i.v.) administration significantly reduced BOLD-weighted fMRI response to forepaw stimulation in somatosensory cortex. In contrast, the fMRI response of the control group showed no significant variations over the duration of the fMRI measurement. The correlation between the decrease in fMRI signal intensity and increase in GABA levels in brain measured using in vivo MRS (Fig. 4) suggests that in acute GABA-T inhibition, the suppression of cortical excitability is related directly to the elevation of cerebral GABA concentration. Our results are in agreement with previous neurochemical studies that have established that GABA-T inhibitors such as vigabatrin and gabaculine raise the overall brain GABA level, as well as those in the nerve endings, accompanied by augmented stimuli-evoked GABA release (Gram et al., 1988; Kihara et al., 1988; Wu et al., 2001).

The findings of the present study therefore suggest that increased availability of endogenous GABA caused by GABA-T inhibition suppresses fMRI signal intensity in α-chloralose-anesthetized rat brain. Although α-chloralose itself has been shown to enhance $GABA_A$ receptor activities (Garrett and Gan, 1998), the statistically significant difference in the time course of fMRI signal intensity between the control group and vigabatrin- and gabaculine-treated groups demonstrated that the observed depression in somatosensory response to forepaw stimulation under α-chloralose anesthesia is caused by

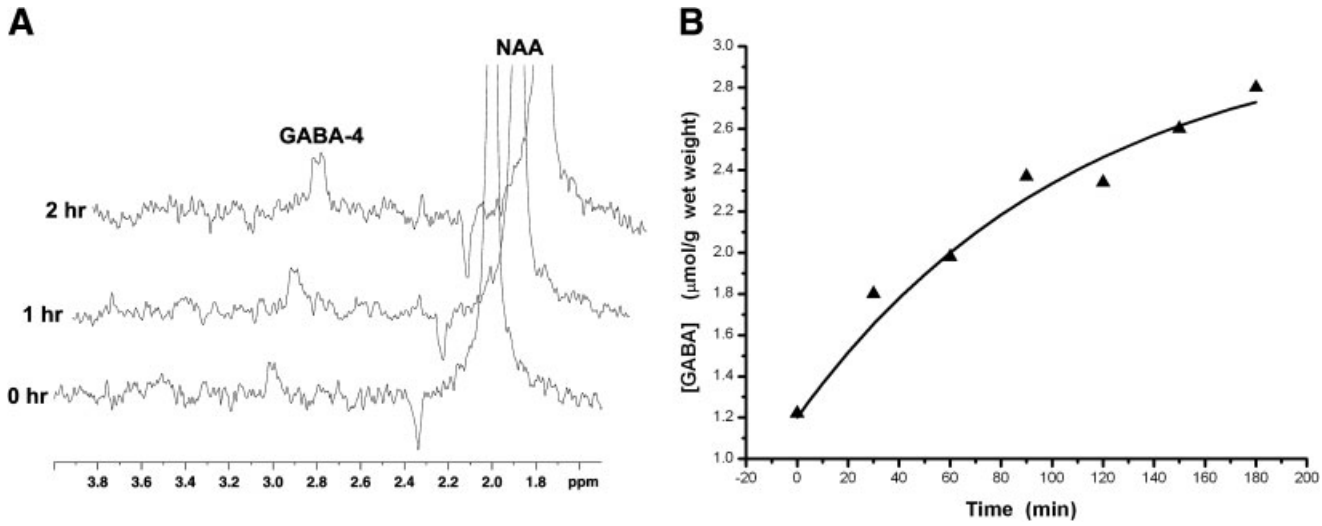

Fig. 3. **A:** Time points from a set of localized homonuclear polarization transfer spectra of GABA-4 methylene protons at 3.0 ppm in the cerebral cortex of α-chloralose-anesthetized rats on acute vigabatrin administration (500 mg/kg, 0.6 cc i.v.; $n = 5$). TR/TE = 2,000/68 msec; voxel size = 4.5 mm × 2.5 mm × 4.5 mm; NS = 256; line-broadening (LB) = 5 Hz). Bottom trace, 0 hr; middle trace, 1 hr; top trace, 2 hr after vigabatrin injection. All spectra were phased using zero-order phase only without any baseline corrections. The same intensity scales were used. **B:** Exponential fit (solid line) to the concentrations of GABA (filled triangle) as a function of time from a vigabatrin-treated rats using equation (1). Halftime $t_{1/2} = 110 \pm 33$ min (mean ± SD, $n = 5$); $[GABA]_\infty = 3.1 \pm 0.7$ μmol/g wet weight (mean ± SD, $n = 5$); $[GABA]_0 = 1.2 \pm 0.1$ μmol/g wet weight (mean ± SD, $n = 11$).

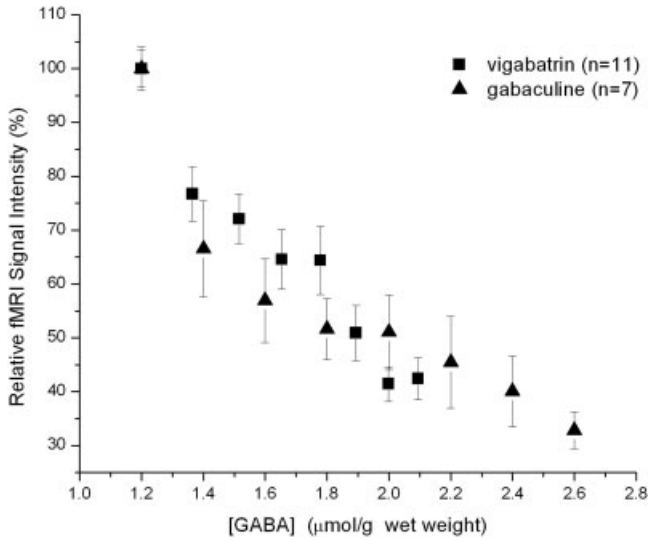

Fig. 4. Correlation between endogenous GABA concentration and fMRI intensity after acute vigabatrin and gabaculine treatment. The concentration of GABA was calculated from the fits to the experimentally determined posttreatment time course of GABA concentration. For vigabatrin treatment, [GABA](t) = (1.2 μmol/g wet weight)(exp[−t/110 min]) + (3.1 μmol/g wet weight)(1 − exp[−t/110 min]) was used. The fMRI intensities of vigabatrin-treated rats are the same as those shown in Figure 2. For gabaculine treatment, [GABA](t) = 1.2 μmol/g wet weight + (0.020 μmol/g wet weight/min)(t) was used.

vigabatrin or gabaculine. The increase in GABA release after GABA-T inhibition has been attributed to a Ca^{2+}-independent process mediated through the reversal in the direction of GABA transporters (Szerb, 1982; Wood et al., 1988; Attwell et al., 1993; Wu et al., 2001, 2003). The following thermodynamic equation has been proposed (Attwell et al., 1993), which describes the dependence of concentration of extracellular GABA ($[GABA]_e$) on that of intracellular GABA ($[GABA]_i$) and the concentrations of Na^+ and Cl^-:

$$[GABA]_e = [GABA]_i([Na^+]_i/[Na^+]_e)^2 \times ([Cl^-]_i/[Cl^-]_e)\exp(VF/RT) \quad (2)$$

where V is the membrane potential, F is Faraday's constant, R is the gas constant, and T is the absolute temperature. During repetitive stimulation (e.g., the forepaw stimulation at a frequency of 3 Hz used in this study), which leads to increased $[Na^+]_i$, the elevated $[GABA]_i$ due to GABA-T inhibition would generate a condition allowing for an increase in the reversal of GABA transporters, leading to increased transporter-mediated GABA release. In hippocampal slices from rats, electrical stimulation at the frequency range of 2.5–10 Hz causes activity-dependent depression of GABA-mediated inhibition that has been shown to be reversed when the rats were pretreated with vigabatrin (Jackson et al., 2000). The correlation observed here of the reduction in fMRI signal intensity, due presumably to augmented GABA-mediated inhibition with elevated endogenous GABA concentra-

tion resulting from GABA-T inhibition, is therefore consistent with previous electrophysiologic studies (Attwell et al., 1993) and could be explained by the mechanism of GABA-T inhibition-induced reversal of GABA transporters (Szerb, 1982; Wood et al., 1988; Wu et al., 2001, 2003).

Because vigabatrin is structurally analogous to GABA and so as to act as a suicide inhibitor of GABA-T (Jung et al., 1977), vigabatrin could also interact with GABAergic neurotransmission at other sites. Previous studies have suggested that vigabatrin also has a secondary inhibitory effect on GABA reuptake (Jackson et al., 1994, 2000). In addition to increasing GABA release, inhibition of GABA uptake itself also leads to augmentation of GABA-mediated synaptic inhibition (Iadarola and Gale, 1981; Golan et al., 1996; Angehagen et al., 2003). Although not demonstrated specifically, gabaculine (also a structural analogue of GABA) (Rando, 1977) therefore may similarly influence GABA neurotransmission. The secondary effects of vigabatrin and possibly of gabaculine on GABA reuptake should also have contributed to the observed correlation in the present acute GABA-T inhibition study (see Fig. 4). For anticonvulsant agents such as valproate and tiagabine that do not cause an overall elevation of GABA concentration (Gram et al., 1988; Angehagen et al., 2003), the correlation between cerebral total GABA concentration measured by in vivo MRS and BOLD-weighted fMRI intensity is not expected. Valproate seems to selectively increase the GABA concentration in the synaptic pool (Iadarola and Gale, 1981). Tiagabine is a potent inhibitor of GABA uptake (Angehagen et al., 2003). Their effects on BOLD-weighted fMRI signals have not yet been elucidated.

The exact mechanism by which increased local neuronal activities trigger the increase in rCBF, which is essential to the BOLD effect, remains under investigation. Several mechanisms have been suggested that involve an array of vasodilatory agents: CO_2, H^+, K^+, adenosine, and NO. When administered exogenously, GABA causes vasodilation and increases CBF; however, the endogenous GABA concentration has been shown to be insufficient to affect cerebral microvascular tone (Fergus and Lee, 1997). It is unlikely that the observed reduction in BOLD response after acute GABA-T inhibition is due to focal vasodilation by increased GABA release, which would have caused an increase in the BOLD fMRI signal intensity.

In conclusion, we have shown that vigabatrin and gabaculine, both highly specific inhibitors of GABA-T, causes elevation of endogenous GABA in the rat brain. Brain GABA level is quantified readily using in vivo selective homonuclear polarization transfer spectroscopy. Correlated with the rise in GABA level, the intensity of BOLD-weighted fMRI signals in somatosensory cortex during forepaw stimulation is reduced significantly. The present in vivo fMRI results are consistent with previous neurochemical and neurophysiologic studies of GABA-T inhibition, which has been demonstrated to lead to augmented GABA release (Kihara et al., 1988; Wu et al., 2001) and activity-dependent reinforcement of inhibition (Jackson et al., 2000). Further studies of drugs targeting GABAergic system using whole brain BOLD and chemical shift images of high spatial resolution should facilitate experimental assessment of regional (e.g., in thalamus) significance and differences in the inhibitory processes. In vivo GABA release and reuptake can also be investigated further using MRS to measure the kinetics of ^{13}C-label incorporation into GABA, glutamate, and glutamine through different metabolic pathways (Manor et al., 1996; Patel et al., 2001; Shen et al., 2002b; Waagepetersen et al., 2003).

ACKNOWLEDGMENTS

We thank Dr. A. Koretsky for many helpful discussions, Drs. H. Merkle and S. Li for construction of RF coils, Mr. D. Letizia and Ms. T. Wilson for surgical assistance, and Mr. S. Hou for computer assistance.

REFERENCES

Angehagen M, Ben-Menachem E, Ronnback L, Hansson E. 2003. Novel mechanisms of action of three antiepileptic drugs, vigabatrin, tiagabine, and topiramate. Neurochem Res 28:333–340.

Attwell D, Barbour B, Szatkowski M. 1993. Nonvesicular release of neurotransmitter. Neuron 11:401–407.

Bandettini PA, Jesmanowicz A, Wong EC, Hyde JS. 1993. Processing strategies for time-course data sets in functional MRI of the human brain. Magn Reson Med 30:161–173.

Behar KL, Boehm D. 1994. Measurement of GABA following GABA-transaminase inhibition by gabaculine: a ^1H and ^{31}P NMR spectroscopic study of rat brain in vivo. Magn Reson Med 31:660–667.

Ben-Menachem E, Persson LI, Schechter PJ, Haegele KD, Huebert N, Hardenberg J, Dahlgren L, Mumford JP. 1989. The effect of different vigabatrin treatment regimens on CSF biochemistry and seizure control in epileptic patients. Br J Clin Pharmacol 27(Suppl):79–85.

Bernasconi R, Klein M, Martin P, Christen P, Hafner T, Portet C, Schmutz M. 1988. Gamma-vinyl GABA: comparison of neurochemical and anticonvulsant effects in mice. J Neural Transm 72:213–233.

Buonocore MH, Gao L. 1997. Ghost artifact reduction for echo planar imaging using image phase correction. Magn Reson Med 38:89–100.

Chen Z, Li SS, Yang J, Letizia D, Shen J. 2004. Measurement and automatic correction of high order B_0 inhomogeneity in the rats brain at 11.7 Tesla. Magn Reson Imaging 22:835–842.

Choi IY, Lee SP, Merkle H, Shen J. 2004. Single-shot two-echo technique for simultaneous measurement of GABA and creatine in the human brain in vivo. Magn Reson Med 51:1115–1121.

Dalvi A, Rodgers RJ. 1996. GABAergic influences on plus-maze behaviour in mice. Psychopharmacology (Berl) 128:380–397.

Dimitrijevic D, Whitton PS, Domin M, Welham K, Florence AT. 2001. Increased vigabatrin entry into the brain by polysorbate 80 and sodium caprate. J Pharm Pharmacol 53:149–154.

Errante LD, Petroff OA. 2003. Acute effects of gabapentin and pregabalin on rat forebrain cellular GABA, glutamate, and glutamine concentrations. Seizure 12:300–306.

Fergus A, Lee KS. 1997. GABAergic regulation of cerebral microvascular tone in the rat. J Cereb Blood Flow Metab 17:992–1003.

Garrett KM, Gan J. 1998. Enhancement of gamma-aminobutyric acid A receptor activity by alpha-chloralose. J Pharmacol Exp Ther 285:680–686.

Gernert M, Thompson KW, Löscher W, Tobin AJ. 2002. Genetically engineered GABA-producing cells demonstrate anticonvulsant effects and long-term transgene expression when transplanted into the central piriform cortex of rats. Exp Neurol 176:183–192.

Golan H, Talpalar AE, Schleifstein-Attias D, Grossman Y. 1996. GABA metabolism controls inhibition efficacy in the mammalian CNS. Neurosci Lett 217:25–28.

Gram L, Larsson OM, Johnsen AH, Schousboe A. 1988. Effects of valproate, vigabatrin and aminooxyacetic acid on release of endogenous and exogenous GABA from cultured neurons. Epilepsy Res 2:87–95.

Gruetter R. 1993. Automatic, localized in vivo adjustment of all first- and second-order shim coils. Magn Reson Med 29:804–811.

Hoge RD, Atkinson J, Gill B, Crelier GR, Marrett S, Pike GB. 1999. Linear coupling between cerebral blood flow and oxygen consumption in activated human cortex. Proc Natl Acad Sci USA 96:9403–9408.

Iadarola MJ, Gale K. 1981. Cellular compartments of GABA in brain and their relationship to anticonvulsant activity. Mol Cell Biochem 39:305–329.

Ishikawa K, Watabe S, Goto N. 1983. Laminal distribution of gamma-aminobutyric acid (GABA) in the occipital cortex of rats: evidence as a neurotransmitter. Brain Res 277:361–364.

Jackson MF, Esplin B, Capek R. 2000. Reversal of the activity-dependent suppression of GABA-mediated inhibition in hippocampal slices from gamma-vinyl GABA (vigabatrin)-pretreated rats. Neuropharmacology 39: 65–74.

Jackson MF, Dennis T, Esplin B, Capek R. 1994. Acute effects of gamma-vinyl GABA (vigabatrin) on hippocampal GABAergic inhibition in vitro. Brain Res 651:85–91.

Jasmin L, Rabkin SD, Granato A, Boudah A, Ohara PT. 2003. Analgesia and hyperalgesia from GABA-mediated modulation of the cerebral cortex. Nature 424:316–320.

Jung MJ, Lippert B, Metcalf BW, Bohlen P, Schechter PJ. 1977. Gamma-vinyl GABA (4-amino hex-5-ynoic acid), a new selective irreversible inhibitor of GABA-T: effects on brain GABA metabolism in mice. J Neurochem 29:797–802.

Kihara M, Misu Y, Kubo T. 1988. GABA transaminase inhibitors enhance the release of endogenous GABA but decrease the release of beta-alanine evoked by electrical stimulation of slices of the rat medulla oblongata. Life Sci 42:1817–1824.

Logothetis NK, Pauls J, Augath M, Trinath T, Oeltermann A. 2001. Neurophysiological investigation of the basis of the fMRI signal. Nature 412:150–157.

Loscher W. 1982. Comparative assay of anticonvulsant and toxic potencies of sixteen GABAmimetic drugs. Neuropharmacology 21:803–810.

Manor D, Rothman DL, Mason GF, Hyder F, Petroff OA, Behar KL. 1996. The rate of turnover of cortical GABA from [1-^{13}C]glucose is reduced in rats treated with the GABA-transaminase inhibitor vigabatrin (gamma-vinyl GABA). Neurochem Res 21:1031–1041.

Marota JJ, Mandeville JB, Weisskoff RM, Moskowitz MA, Rosen BR, Kosofsky BE. 2000. Cocaine activation discriminates dopaminergic projections by temporal response: an fMRI study in Rat. Neuroimage 11:13–23.

Martin DL, Rimvall K. 1993. Regulation of gamma-aminobutyric acid synthesis in the brain. J Neurochem 60:395–407.

Mattson RH, Petroff O, Rothman D, Behar K. 1994. Vigabatrin: effects on human brain GABA levels by nuclear magnetic resonance spectroscopy. Epilepsia 35(Suppl):29–32.

McCormick DA. 1989. GABA as an inhibitory neurotransmitter in human cerebral cortex. J Neurophysiol 62:1018–1027.

Miller JM, Jope RS, Ferraro TN, Hare TA. 1990. Brain amino acid concentrations in rats killed by decapitation and microwave irradiation. J Neurosci Methods 31:187–192.

Ogawa S, Lee TM, Stepnoski R, Chen W, Zhu XH, Ugurbil K. 2000. An approach to probe some neural systems interaction by functional MRI at neural time scale down to milliseconds. Proc Natl Acad Sci USA 97: 11026–11031.

Patel AB, Rothman DL, Cline GW, Behar KL. 2001. Glutamine is the major precursor for GABA synthesis in rat neocortex in vivo following acute GABA-transaminase inhibition. Brain Res 919:207–220.

Petroff OA, Behar KL, Mattson RH, Rothman DL. 1996. Human brain gamma-aminobutyric acid levels and seizure control following initiation of vigabatrin therapy. J Neurochem 67:2399–2404.

Pfeuffer J, Tkac I, Provencher SW, Gruetter R. 1999. Toward an in vivo neurochemical profile: quantification of 18 metabolites in short-echo-time ^{1}H NMR spectra of the rat brain. J Magn Reson 141:104–120.

Preece NE, Cerdan S. 1996. Metabolic precursors and compartmentation of cerebral GABA in vigabatrin-treated rats. J Neurochem 67: 1718–1725.

Rando RR. 1977. Mechanism of the irreversible inhibition of gamma-aminobutyric acid-alpha-ketoglutaric acid transaminase by the neurotoxin gabaculine. Biochemistry 16:4604–4610.

Riekkinen PJ, Pitkanen A, Ylinen A, Sivenius J, Halonen T. 1989. Specificity of vigabatrin for the GABAergic system in human epilepsy. Epilepsia 30(Suppl):18–22.

Schechter PJ, Sjoerdsma A. 1990. Clinical relevance of measuring GABA concentrations in cerebrospinal fluid. Neurochem Res 15:419–423.

Schousboe A. 1990. Neurochemical alteration associated with epilepsy or seizure activity. In: Dam M, Gram L, editors. Comprehensive epileptology. New York: Raven Press. p 1–16.

Shen J, Rothman DL, Hetherington HP, Pan JW. 1999a. Linear projection method for automatic slice shimming. Magn Reson Med 42:1082–1088.

Shen J. 2003. Slice-selective J-coupled coherence transfer using symmetric linear phase pulses: applications to localized GABA spectroscopy. J Magn Reson 163:73–80.

Shen J, Rothman DL, Brown P. 2002a. In vivo GABA editing using a novel doubly selective multiple quantum filter. Magn Reson Med 47: 447–454.

Shen J, Rothman DL. 2002b. Magnetic resonance spectroscopic approaches to studying neuronal: glial interactions. Biol Psychiatry 52: 694–700.

Shen J, Shungu DC, Rothman DL. 1999b. In vivo chemical shift imaging of γ-aminobutyric acid in the human brain. Magn Reson Med 41:35–42.

Shen J, Yang J, Choi IY, Li SS, Chen Z. 2004. A new strategy for in vivo spectral editing. Application to GABA editing using selective homonuclear polarization transfer spectroscopy. J Magn Reson 170: 290–298.

Sherif F, Harro J, el-Hwuegi A, Oreland L. 1994. Anxiolytic-like effect of the GABA-transaminase inhibitor vigabatrin (gamma-vinyl GABA) on rat exploratory activity. Pharmacol Biochem Behav 49:801–805.

Silva AC, Koretsky AP. 2002. Laminar specificity of functional MRI onset times during somatosensory stimulation in rat. Proc Natl Acad Sci USA 99:15182–15187.

Silva AC, Lee SP, Yang G, Iadecola C, Kim SG. 1999. Simultaneous blood oxygenation level-dependent and cerebral blood flow functional magnetic resonance imaging during forepaw stimulation in the rat. J Cereb Blood Flow Metab 19:871–879.

Silva AC, Zhang W, Williams DS, Koretsky AP. 1995. Multi-slice MRI of rat brain perfusion during amphetamine stimulation using arterial spin labeling. Magn Reson Med 33:209–214.

Spanaki MV, Siegel H, Kopylev L, Fazilat S, Dean A, Liow K, Ben-Menachem E, Gaillard WD, Theodore WH. 1999. The effect of vigabatrin (gamma-vinyl GABA) on cerebral blood flow and metabolism. Neurology 53:1518–1522.

Szerb JC. 1982. Turnover and release of GABA in rat cortical slices: effect of a GABA-T inhibitor, gabaculine. Neurochem Res 7:191–204.

Tappaz ML, Brownstein MJ, Kopin IJ. 1977. Glutamate decarboxylase (GAD) and gamma-aminobutyric acid (GABA) in discrete nuclei of hypothalamus and substantia nigra. Brain Res 125:109–121.

van Zijl PC, Eleff SM, Ulatowski JA, Oja JM, Ulug AM, Traystman RJ, Kauppinen RA. 1998. Quantitative assessment of blood flow, blood volume and blood oxygenation effects in functional magnetic resonance imaging. Nat Med 4:159–167.

Waagepetersen H, Sonnewald U, Schousboe A. 2003. Compartmentation of glutamine, glutamate, and GABA metabolism in neurons and astrocytes: functional implications. Neuroscientist 9:398–403.

Wood JD, Geddes JW, Tsui SK, Kurylo E. 1982. Combined effects of a metabolic inhibitor (gabaculine) and an uptake inhibitor (ketamine) on the gamma-aminobutyrate system in mouse brain. J Neurochem 39: 1710–1715.

Wood JD, Kurylo E, Lane R, Geddes JW, Tsui SK. 1988. Gamma-aminobutyric acid release from synaptosomes prepared from rats treated with isonicotinic acid hydrazide and gabaculine. J Neurochem 50:1839–1843.

Wu Y, Wang W, Richerson GB. 2001. GABA transaminase inhibition induces spontaneous and enhances depolarization-evoked GABA efflux via reversal of the GABA transporter. J Neurosci 21:2630–2639.

Wu Y, Wang W, Richerson GB. 2003. Vigabatrin induces tonic inhibition via GABA transporter reversal without increasing vesicular GABA release. J Neurophysiol 89:2021–2034.